

## Anti-Stokes luminescence in chromium-doped ZnSe

V. Yu. Ivanov

*Dnepropetrovsk State University, Dnepropetrovsk, Ukraine*

Yu. G. Semenov

*Institute of Semiconductor Physics, Ukrainian Academy of Sciences, Kiev, Ukraine*

M. Surma and M. Godlewski

*Institute of Physics, Polish Academy of Sciences, Warsaw, Poland*

(Received 21 August 1995; revised manuscript received 19 January 1996)

The results of comprehensive studies of photoluminescence, photoluminescence excitation, electron spin resonance, and photoconductivity of chromium-doped ZnSe are discussed. It is shown that the blue anti-Stokes luminescence of ZnSe:Cr is induced by the two-step ionization transitions of Cr in which the charge state of chromium is changed from 2+ to 1+ and from 1+ to 2+. We also propose that some cooperative processes can contribute to excitation of the anti-Stokes luminescence. The Auger-type energy transfer mechanism of the photoluminescence excitation is discussed. [S0163-1829(96)03728-9]

### I. INTRODUCTION

In some cases photoluminescence (PL) emission is observed for light energies larger than the excitation energy. Such phenomenon we call anti-Stokes luminescence (ASL). During the last few decades the ASL was observed in different media—in metal vapors, for organic molecules, in dielectric crystals activated with rare-earth (RE) ions, and in semiconductor crystals.<sup>1-7</sup> A particular interest represents the study of ASL in solids where an anti-Stokes shift considerably exceeds vibrational energy of the lattice. In some cases it can reach a value of about 1 eV.

The ASL has found several practical applications. For example, investigations of the ASL in dielectric crystals activated with RE ions, carried out in the 1960s, led to the introduction of the anti-Stokes luminophors.

The ASL of RE ions and of F centers was explained by the cooperative luminescence mechanism.<sup>3-5</sup> For semiconductors the ASL was first observed for CdS.<sup>2</sup> Two mechanisms were proposed to explain the ASL in semiconductors. The first of them explains excitation of the ASL by multiphoton absorption, which may occur upon high density of excitation. The second, expected also for a low and moderate density of excitation, assumes a two-step electronic transition of a carrier from a valence band (VB) to a conduction band (CB) proceeding via some deep impurity (defect) level. Free carriers are created in the VB and CB in two complementary photoionization transitions. The ASL can then be observed consisting of band-to-band, excitonic, and donor-acceptor pair (DAP) recombination transitions.

Recently, the ASL was reported for the range of the Cd<sub>1-x</sub>Zn<sub>x</sub>S mixed crystals by Carlone, Beliveau, and Rowell.<sup>7</sup> These authors have shown that the spectral characteristics of the effect depend on impurities present in the samples. This is expected for the second mechanism of the ASL excitation.

In this work we report the observation of the ASL in chromium-doped ZnSe. Properties of the ASL are discussed

and the ASL emission is explained by the two-step ionization transitions of chromium ions in the ZnSe lattice. We suggest that at increased excitation density, complicated cooperative transitions of chromium ion and donor-acceptor pairs can be important.

### II. EXPERIMENTAL SETUP

ZnSe crystals studied were grown from melt by the Bridgman-Stockbarger method and were purified by a zone melting with the following treatment in a zinc melt. The samples were intentionally doped with chromium, which was introduced to the melt. Chromium concentration, determined from the mass spectral analysis, varied between 10<sup>16</sup> and 5×10<sup>19</sup> cm<sup>-3</sup>. The concentration of unintentional impurities, such as Cu, Mn, Fe, Cl, Na, and Li was below 10<sup>16</sup> cm<sup>-3</sup>. The samples had the shape of a rectangular prism of 4×4×2 mm dimension and were oriented either in (111) or (110) planes.

Several laser systems were used for the PL excitation. The 2.807-eV line of a helium-cadmium, all “visible” lines and 3.405-eV UV line of a coherent argon-ion and Rodamine R-6G and Oxazin ON-110 dye (1.65–2.25-eV) lasers were used for the photoexcitation. Light intensity was varied in the range of 6×10<sup>16</sup>–10<sup>19</sup> photons/(cm<sup>2</sup> s) using a polarization attenuator. The laser beam was typically focused to a spot of 75 μm diameter.

The PL and photoconductivity spectra were measured with samples mounted in the temperature variable cryostat working between 4.2 and 300 K. The light was dispersed with either MDD 500×2 (Czerny-Turner type) or GDM 1000 double grating monochromators with a maximal spectral resolution of 3×10<sup>-5</sup> eV. The electron spin resonance (ESR) experiments were performed on either SE/X-2542 or Bruker 418s and Bruker 300 X-band spectrometers equipped with a continuous He gas-flow Oxford Instruments cryostat.

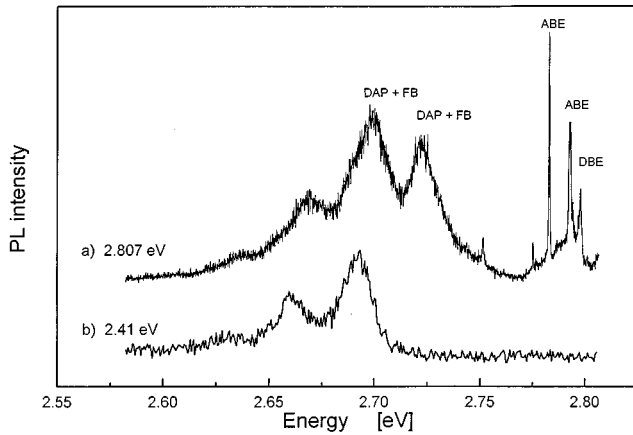


FIG. 1. Photoluminescence spectrum of the ZnSe:Cr ( $4 \times 10^{18} \text{ cm}^{-3}$ ) measured at 4.2 K under the near band-to-band (2.807 eV) and 2.41-eV photoexcitations.

Photoexcitation of the samples mounted in a microwave cavity was done either with laser sources used in the PL study or with a high-pressure mercury lamp and set of interference filters. An electrometric amplifier was used for measuring electrical conductivity, detecting currents in the range of  $10^{-10}$ – $10^{-5}$  A.

### III. EXPERIMENTAL RESULTS

In Fig. 1 we show the PL spectrum of the ZnSe:Cr measured at 4.2 K for two different (2.807 and 2.41 eV) photon energies of the photoexcitation. The PL spectrum under 2.807-eV excitation, i.e., under near band-to-band excitation ( $E_G = 2.82$  eV), consists of three sharp emission lines at 2.7977, 2.7930, and 2.7829 eV, which are due to a radiative recombination of neutral donor (Al?) bound excitons<sup>8</sup> (DBE) and two acceptor bound excitons' (ABE) emission at 2.7930 eV [Na? (Ref. 8)] and 2.7829 eV.<sup>8</sup> Two weak structures observed at lower energies can likely be attributed to either LO-phonon or so-called two-electron (hole) ( $2s$ ) replica of the excitonic emissions. The excitonic emissions were also observed for excitation with photon energies above the ZnSe band-gap energy ( $E_G$ ).

In addition, we observed a structured PL emission between 2.62 and 2.75 eV. This part of the spectrum consists, for the 2.807-eV excitation, of the superimposed free (electron)-to-bound (shallow acceptor) (FB) and shallow-donor–shallow-acceptor pair transitions with zero phonon lines (ZPL) at about 2.720 and 2.692 eV and their LO-phonon replica. The 2.692-eV PL can be attributed to the radiative decay of an electron on a shallow donor (Ga or Al) and a hole on a shallow acceptor [Li (Refs. 9 and 10)]. This PL showed a strong dependence on excitation intensity (DAP part of the spectrum shifts towards higher energy) and on temperature and was observed for the excitation energies larger than 2.0 eV. In Fig. 2 we show the excitation spectrum (PL intensity versus photon energy of the excitation) of the “shallow” DAP PL with the ZPL at 2.692 eV. The 2.692 eV is observed for excitation with photon energies larger than 2.0 eV, i.e., smaller energies than the emission energy. This PL will later be called the ASL emission. At 4.2 K the shape of the ASL PL is not dependent on the excitation energy.

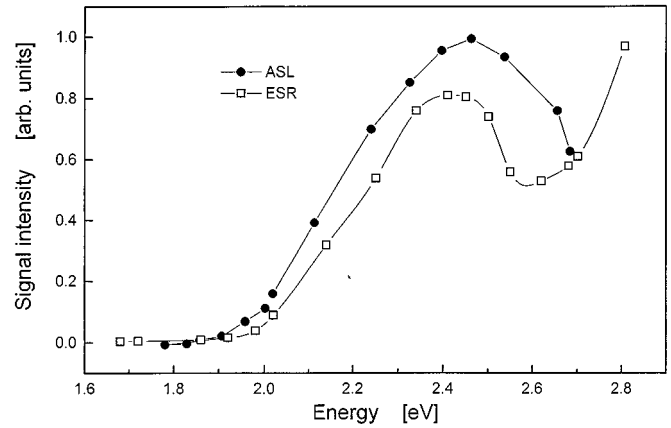


FIG. 2. Excitation spectra of the shallow-donor–shallow-acceptor pair photoluminescence (ZPL at 2.692 eV, labeled as the ASL emission) (a) and of the photosensitive ESR signal of the  $\text{Cr}^{1+}$  (b) in the ZnSe:Cr ( $4 \times 10^{18} \text{ cm}^{-3}$ ).

However, with rising temperature the DAP ASL emission is deactivated (thermal ionization of shallow donors) and free-to-bound PL becomes dominant at temperatures above 60 K.

The dependence of the ASL intensity on the excitation density was measured (Fig. 3). The data shown in Fig. 3 were measured for the excitation intensity varied between about  $10^{16}$  and  $10^{19}$  photons/( $\text{cm}^2 \text{ s}$ ). At lower intensities the ASL emission was not observed, whereas, for the excitation densities above  $10^{19}$  photons/( $\text{cm}^2 \text{ s}$ ) the two-photon excitation processes become important. The quadratic dependence is observed at lower excitation density [below  $10^{17}$  photons/( $\text{cm}^2 \text{ s}$ )], which is followed by the linear dependence observed at increased excitation intensities.

In addition to the “shallow” DAP ASL emission the well-known red and green DAP emissions were observed (Fig. 4). The relative intensity of the red and green DAP PL emissions critically depended on the energy of the excitation. Intensity of the two DAP PLs was relatively low, which is due to a high concentration of the Cr in our samples. Chro-

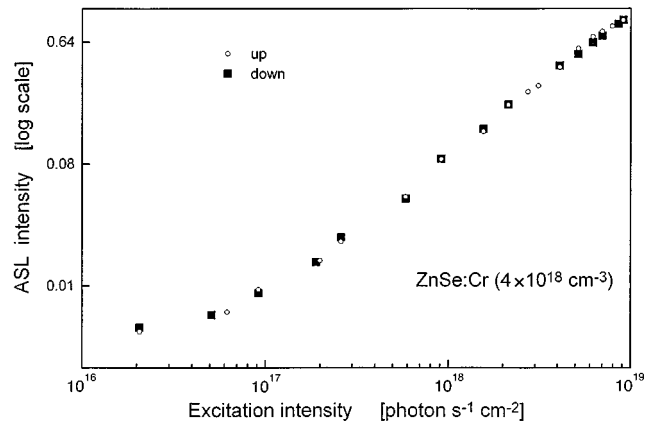


FIG. 3. Dependence of the ASL intensity (shallow-donor–shallow-acceptor pair recombination with ZPL at 2.692 eV) on the excitation intensity. The quadratic dependence is observed at lower light intensities [about  $10^{17}$  photons/( $\text{cm}^2 \text{ s}$ )] followed by a linear one at increased light intensity [below  $10^{19}$  photons/( $\text{cm}^2 \text{ s}$ )]. The spectrum was measured at 4.2 K for increasing (up) and decreasing (down) light intensities to avoid possible hysteresis effects.

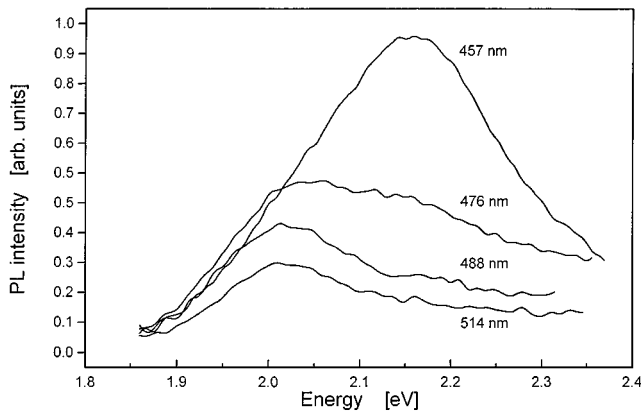


FIG. 4. Visible part of the photoluminescence spectrum of the ZnSe:Cr ( $4 \times 10^{18} \text{ cm}^{-3}$ ) for four different excitation energies and 4.2-K temperature. The overlapping red and green donor-acceptor pair recombination transitions are observed.

mium and other transition-metal dopants are efficient centers of nonradiative recombination.<sup>11</sup>

In the ESR study we have observed (in the dark) a weak spectrum of the  $\text{Mn}^{2+}$ . Two further ESR signals were observed under the photoexcitation. These were the relatively weak ESR signal of the  $\text{Fe}^{3+}$  and the strong ESR signal of  $\text{Cr}^{1+}$ . In Fig. 2 we show the excitation spectrum of the ESR signal of the  $\text{Cr}^{1+}$ . This spectrum is compared with the excitation spectrum of the ASL emission, which is also shown in Fig. 2, and with the photoconductivity (PC) spectrum of the ZnSe:Cr depicted in Fig. 5. The PC spectrum is shown for three different temperatures  $-5$ ,  $40$ , and  $100 \text{ K}$ .

#### IV. DISCUSSION

As was discussed in the Introduction, two mechanisms were proposed to account for the ASL in semiconductors. These were the multiphoton transition and the two-step ionization transition via some deep trap center. As will be discussed below, we favor the latter explanation of the ASL process in ZnSe:Cr. As will be indicated later, we also believe that some cooperative transitions can contribute to the

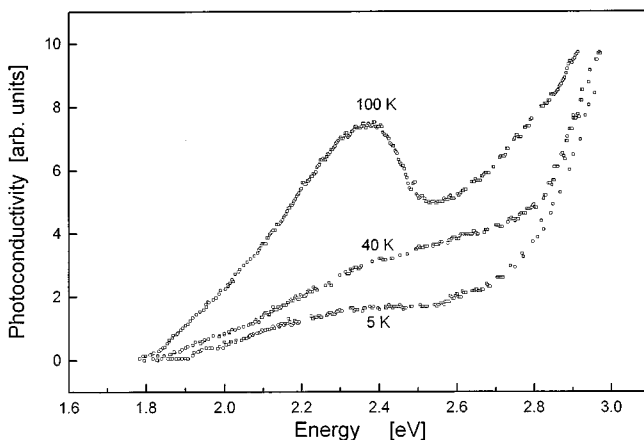


FIG. 5. Photoconductivity spectrum of the ZnSe:Cr ( $4 \times 10^{18} \text{ cm}^{-3}$ ) measured at three different temperatures.

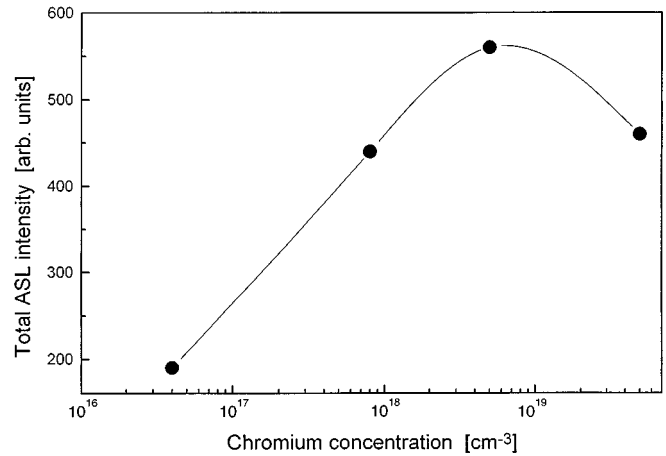


FIG. 6. Dependence of the intensity of the ASL emission on chromium concentration in ZnSe:Cr samples measured at 4.2 K. To minimize error of relative intensities of the ASL emission the samples were mounted together on the sample holder and a fixed excitation (2.41-eV photon energy) intensity was used. Cr concentration in the samples was determined from the mass spectral analysis. The estimated experimental error is within the size of data points.

observed ASL and the visible and infrared PL emissions of ZnSe:Cr. These processes will be discussed in Sec. IV C.

#### A. Mechanism of the anti-Stokes PL

Comparison of the ASL and ESR excitation spectra shown in Fig. 2 and of the photoconductivity spectrum shown in Fig. 5 clearly favors the two-step excitation mechanism of the “edge” PL in ZnSe:Cr. The ASL is excited by the  $2+ \rightarrow 1+$  photoionization transition of chromium, which occurs for the photon energies larger than about 2 eV. Such identity of the ESR excitation band was proved in the previous ESR experiments.<sup>12</sup> The  $2+/1+$  energy level of Cr lies about 2 eV above the VB edge of ZnSe.<sup>12</sup> Once the  $\text{Cr}^{1+}$  state is populated, the complementary  $1+ \rightarrow 2+$  transition can take place. Recent ESR studies of Cr-doped ZnSe,<sup>12</sup> ZnS,<sup>13</sup> and iron-doped ZnSe (Ref. 14) and ZnS (Ref. 15) confirmed relatively high efficiency of the complementary ionization transitions. Moreover, it was observed that two-step ionization transitions of these two ions result in a population of both shallow donors and shallow and deep acceptors.<sup>16</sup> In the  $2+ \rightarrow 1+$  transition free holes (first step) and in the  $1+ \rightarrow 2+$  transition free electrons (second step) are created. These free carriers can then participate in the PL recombination transitions resulting in the appearance of the ASL.

For the two-step excitation process the ASL intensity should depend on the Cr concentration in the sample. In fact such dependence is observed, as is shown in Fig. 6. Only a weak ASL emission is observed in the lightly doped sample (about  $10^{16} \text{ cm}^{-3}$ ) and its intensity increases by a factor 4–5 with increasing Cr concentration. For samples with Cr concentration up to  $5 \times 10^{18} \text{ cm}^{-3}$  this increase is approximately linear. Then this trend saturates and the ASL emission decreases in the intensity for Cr concentration above  $10^{19} \text{ cm}^{-3}$ , which is likely an evidence of the enhanced nonradiative recombination in such samples.<sup>11</sup>

Formally, for the two-step ionization process we should observe quadratic dependence of the ASL intensity on the excitation density. However, such dependence was observed for only low excitation density and the linear dependence was observed for higher intensity of the photoexcitation. The two-step ASL process can be described by the set of the simple kinetics equations, given below, which we introduce to describe the dependence of the ASL intensity (at low temperature) on excitation density:

$$\frac{dn_{\text{Cr}}}{dt} = I\sigma_{OV}(N_{\text{Cr}} - n_{\text{Cr}}) - I\sigma_{OC}n_{\text{Cr}} + n(N_{\text{Cr}} - n_{\text{Cr}})c_{\text{Cr}}^e - pn_{\text{Cr}}c_{\text{Cr}}^h - \beta_{\text{ACr}}n_{\text{A}}n_{\text{Cr}}, \quad (1)$$

$$\frac{dn}{dt} = I\sigma_{OC}n_{\text{Cr}} - n(N_{\text{D}} - n_{\text{D}})c_{\text{D}}^e - n(N_{\text{Cr}} - n_{\text{Cr}})c_{\text{Cr}}^e, \quad (2)$$

$$\frac{dp}{dt} = I\sigma_{OV}(N_{\text{Cr}} - n_{\text{Cr}}) - p(N_{\text{A}} - n_{\text{A}})c_{\text{A}}^h - pn_{\text{Cr}}c_{\text{Cr}}^h, \quad (3)$$

$$\frac{dn_{\text{A}}}{dt} = p(N_{\text{A}} - n_{\text{A}})c_{\text{D}}^e - \beta_{\text{AD}}n_{\text{A}}n_{\text{D}} - \beta_{\text{ACr}}n_{\text{A}}n_{\text{Cr}}, \quad (4)$$

$$\frac{dn_{\text{D}}}{dt} = n(N_{\text{D}} - n_{\text{D}})c_{\text{D}}^e - \beta_{\text{AD}}n_{\text{A}}n_{\text{D}}, \quad (5)$$

where  $n_{\text{Cr}}$  and  $N_{\text{Cr}}$  are the concentration of the chromium in the 1+ charge state and the total concentration of Cr in the sample, respectively.  $N_{\text{A}}$  and  $N_{\text{D}}$  are the total concentrations of acceptors (A) and donors (D) in the sample, and  $n_{\text{A}}$  and  $n_{\text{D}}$  are the concentrations of populated (neutral) acceptors and donors.  $n$ ,  $p$  are the concentrations of free electrons in the CB and free holes in the VB.  $\sigma_{OC}$  and  $\sigma_{OV}$  are the optical ionization rates for the two complementary ionization transitions of Cr. By  $c_{\text{D}}^e$ ,  $c_{\text{A}}^h$ ,  $c_{\text{Cr}}^e$ , and  $c_{\text{Cr}}^h$  we denote capture rates of electrons ( $e$ ) by ionized donors, holes ( $h$ ) by ionized acceptors, and electrons by  $\text{Cr}^{2+}$  and holes by  $\text{Cr}^{1+}$ . By  $\beta_{\text{DAP}}$  we describe an average rate of the DAP recombination, by  $\beta_{\text{ACr}}$   $\text{Cr}^{1+}$ -acceptor tunneling, and  $I$  stands for the light intensity of the photoexcitation.

Several approximations were introduced to Eqs. (1)–(5). We do not consider radiative capture of electrons by acceptors and holes by donors. The data shown in Figs. 1 and 5 indicate that such capture processes are rather inefficient at 4.2-K temperature. Moreover, since the  $\text{Fe}^{3+}$  ESR was relatively weak, we do not introduce electron and hole recombination via Fe and ZnSe even though iron is an efficient center of nonradiative recombination in the ZnSe.<sup>14</sup> We also assumed (for simplicity only) that only one type of shallow donor and shallow acceptors participates in the DAP recombination transitions. Finally, we introduced an average rate of the DAP recombination and Cr-acceptor tunneling, even though such rates should depend on a distance between donor, chromium, and acceptor. The latter is rather a common approximation.

Introducing the neutrality condition, finding a solution at equilibrium, and assuming that the free-carrier concentration is small at low temperature we can obtain the following formula describing intensity of the DAP ASL:

$$I_{\text{PL}} \approx \text{const} \times IN_{\text{Cr}}, \quad (6)$$

either when shallow acceptors dominate over  $\text{Cr}^{1+}$  in hole capture processes or when  $\text{Cr}^{1+}$ -acceptor tunneling becomes efficient. The former case is rather unlikely considering high Cr concentration in our crystals. Linear dependence is also expected for the Auger-type cooperative process discussed later. We do not know which of these mechanisms dominates in our case.

## B. Recombination transitions in ZnSe:Cr

We should explain why quite different PL emissions are observed for the band-to-band excitation and for the excitation within the Cr ionization band (Fig. 1). For the band-to-band excitation several excitonic and shallow DAP bands are observed. This allows us to identify shallow donor and acceptor species present in the samples studied. The PL spectrum indicates a presence of one type of shallow donors in our crystals (Al or Ga). The DBE emission at 2.7977 eV is attributed to the radiative decay of bound excitons at neutral aluminum donor.<sup>8</sup> The Al donor has the 25–26-meV thermal ionization energy.<sup>8</sup> The ABE PL emission at 2.7930 eV may be attributed to a radiative transition of either the Na (Ref. 8) or Li (Ref. 10) [shallow acceptors with 90–100-meV (Na) or 114-meV (Li) ionization energies<sup>10</sup>] bound exciton. The identity of the 2.7829-eV ABE emission is not clear. The free-to-bound emission had its zero phonon line at about 2.720 eV. This allows us to estimate thermal ionization energy of the shallow acceptor center participating in this and “shallow” DAP transitions for 112 meV, which agrees with thermal ionization energy of  $\text{Li}_{\text{Zn}}$  shallow acceptors contributing also to the excitonic part of the PL. Also the DAP PL emission with a zero phonon line at about 2.692 eV agrees well with the spectral position of the shallow-donor (Ga or Al)–Li-acceptor transition.<sup>9,10</sup>

The observed complex PL emission can thus be explained by the presence of at least one type of shallow donors (Al or Ga) and two shallow acceptors (Na or Li and an unidentified) in our crystals. The puzzling result is why a contribution of different excitonic and free-to-bound and DAP PL transitions so critically depends on the excitation energy. The bound excitons are observed only under the direct band-to-band excitation. They are not created if free electrons and holes are excited separately in two-step processes via the Cr ion. For nearly resonant band-to-band photoexcitation electron-hole pairs may readily form free excitons, which can then be trapped by neutral donor and acceptor centers. This results in a formation of donor and acceptor bound excitons. The DBEs and ABEs can also be formed by a subsequent trapping of electrons and holes. We expect that this mechanism of the DBE and ABE formation is less efficient since DBE and ABE PL emissions were not observed upon two-step photoexcitation.

The separately excited free carriers are trapped by shallow donors and acceptors and recombine before the next carriers will be available for bound exciton formation. This is confirmed by the PC measurements shown in Fig. 5. A pronounced PC signal is observed only at increased temperature, when shallow trap centers are thermally ionized. This also explains why we have not observed the band-to-band PL emission. We also expect that Cr can successfully compete

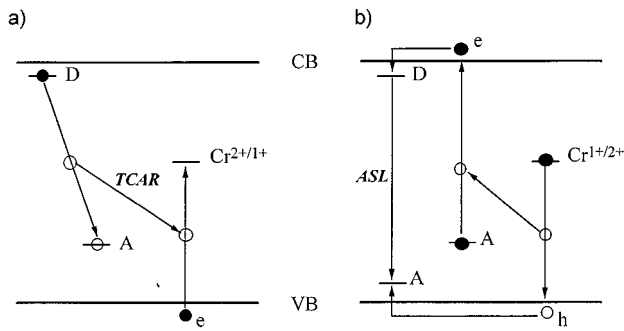


FIG. 7. Model of the three-center Auger recombination (TCAR) transition and of a quasisonant excitation of the red DAP PL in ZnSe:Cr ( $4 \times 10^{18} \text{ cm}^{-3}$ ) by the Auger-type energy transfer from recombining  $\text{Cr}^{1+}$  ion.

with shallow centers in carrier trapping processes, as was also concluded from our recent ESR studies.<sup>12</sup>

The efficiency of the red<sup>17</sup> and green<sup>18</sup> DAP emissions of ZnSe also depended on the excitation energy. When deep acceptors were not directly ionized, the red DAP PL, due to the 0.7-eV-deep (zinc vacancy-donor,  $V_{\text{Zn}}-D$ ) complex acceptor,<sup>19,20</sup> dominated. Green DAP PL, due to the 0.4-eV-deep Cu- $D$  complex acceptor,<sup>19,20</sup> appears only under direct photoionization of the 0.4-eV acceptor. This property of the DAP PL can tentatively be explained by larger hole trapping rates for the 0.7-eV-deep acceptor than for the 0.4-eV acceptor, but later we will propose another possible explanation of this result.

### C. Cooperative Cr-DAP transitions

Here below we will propose two cooperative transitions which may account for our experimental results. The mechanisms discussed are rather tentative and further experimental evidence is required to prove their efficiency.

The first process is an Auger-type recombination of the DAP, the process in which the recombination energy of the DAP is transferred to the nearby Cr center. The three-center Auger recombination is explained in Fig. 7. The recombination energy of the DAP is used for the ionization of deep trap center due to the transition-metal (TM) ion, i.e., three centers participate in the energy transfer process. Three-center Auger transitions were observed previously for the Fe centers in the ZnS,<sup>21,22</sup> and recently in the ZnSe. The theoretical estimation of the Auger recombination rate indicated that the process should take place for only relatively close DAP-deep-center associates.<sup>22</sup> For such associates the reverse process, i.e., the TM ion recaptures a carrier and an excess energy is used for the DAP excitation, should also be possible. In fact the matrix elements for this transition are identical to that of the three-center Auger recombination (TCAR) process. Such reverse transition was not observed till now. For Fe in ZnS the DAP recombination energy is larger than the Fe-CB energy

distance. In consequence, electrons ionized from Fe centers are excited high into continuum of the CB states. They rapidly thermalize their excess energy, making the reverse process impossible (electron- $\text{Fe}^{3+}$  energy is too small for the direct excitation of the associated DAP).

We indicate here that a different situation occurs for the Cr ion in the ZnSe. The  $2+ \rightarrow 1+$  ionization energy of Cr in ZnSe is nearly resonant with the DAP excitation energy for the red PL emission. We indicate here that the mechanism discussed in Fig. 7 can also lead to the ASL excitation [see Fig. 7(b)]. For close DAP-Cr associates, expected in our heavily Cr-doped samples, hole retrapping by  $\text{Cr}^{1+}$  may result in the quasisonant excitation of the red DAP PL. This may explain why the red DAP PL dominates over the green DAP PL under the excitation with photon energies within the Cr ionization band. The ASL emission can appear if part of the photoexcited holes does not recombine with  $\text{Cr}^{1+}$  centers and is trapped by shallow acceptors. Then, electrons photoinduced in the ionization transition of deep acceptors (see Fig. 7) and trapped at shallow donors can recombine with holes on shallow acceptors, i.e., the ASL can be observed. The complementary  $\text{Cr} \rightarrow \text{CB}$  transition is then not necessary to get the ASL. Linear dependence of the ASL on the excitation intensity is expected for such excitation mechanism of the ASL.

For increased population of active centers (Cr associated with DAPs)  $\text{Cr}^{1+}$ -acceptor tunneling transitions should also take place. Such deep center-acceptor tunneling transitions were observed in several cases (e.g., Ref. 23). Such transitions should also occur for Cr centers and shallow donors. If tunneling transitions are included in Eqs. (1)–(5) the  $I^2$  dependence of the  $I_{\text{ASL}}$  should be observed only at low excitation intensities. For increased concentrations of  $\text{Cr}^{1+}$  and populated acceptors the tunneling process starts to be efficient and linear dependence  $I_{\text{ASL}} \approx I$  should occur, as in fact is observed by us.

## V. CONCLUSIONS

The anti-Stokes PL in ZnSe:Cr is explained by the ionization transitions of the Cr ion resulting in subsequent creation of free holes in the VB and electrons in the CB. We indicate, however, that the cooperative transitions can also contribute to the ASL. The Auger-type energy transfer from DAPs to Cr and a reverse process can lead to the ASL emission induced by only  $\text{Cr}^{2+} \rightarrow \text{Cr}^{1+}$  ionization of Cr. The linear dependence of the ASL intensity on the excitation density is then expected. Efficient Cr-acceptor tunneling can also explain the observed linear dependence of the ASL intensity on the excitation density.

## ACKNOWLEDGMENT

The work was partially supported by Grant No. U68000 from the International Science Foundation.

- <sup>1</sup>E. F. Apple, J. Electrochem. Soc. **116**, 120 (1969).
- <sup>2</sup>R. E. Halsted, E. F. Apple, and J. S. Prener, Phys. Rev. Lett. **2**, 420 (1959).
- <sup>3</sup>D. L. Dexter, Phys. Rev. **126**, 1962 (1962).
- <sup>4</sup>P. P. Feofilov and V. V. Ovsyankin, Appl. Opt. **6**, 1828 (1967).
- <sup>5</sup>I. Broser and R. Broser-Warminsky, in *Proceedings of the International Conference on the Luminescence of Organic and Inorganic Materials* (New York, 1962), p. 402.
- <sup>6</sup>B. Clerjaud, F. Gendron, and C. Porte, J. Lumin. **24/25**, 277 (1981).
- <sup>7</sup>C. Carlone, A. Beliveau, and N. L. Rowell, J. Lumin. **47**, 309 (1991).
- <sup>8</sup>P. J. Dean, D. C. Herbert, C. J. Werkhoven, B. J. Fitzpatrick, and R. N. Bhargava, Phys. Rev. B **23**, 4888 (1981).
- <sup>9</sup>V. Swaminathan and L. C. Green, Phys. Rev. B **14**, 5351 (1976).
- <sup>10</sup>J. L. Merz, K. Nassau, and J. W. Shiever, Phys. Rev. B **8**, 1444 (1973).
- <sup>11</sup>M. Godlewski and A. Zakrzewski, in *II-VI Semiconductors*, edited by M. Jain (World Scientific, Singapore, 1993), p. 205.
- <sup>12</sup>M. Godlewski and M. Kamińska, J. Phys. C **13**, 6537 (1980).
- <sup>13</sup>M. Godlewski, Z. Wilamowski, M. Kamińska, W. E. Lamb, and B. C. Cavenett, J. Phys. C **14**, 2835 (1981).
- <sup>14</sup>M. Surma, M. Godlewski, and T. P. Surkova, Phys. Rev. B **50**, 8319 (1994).
- <sup>15</sup>M. Godlewski and A. Zakrzewski, J. Phys. C **18**, 6615 (1985).
- <sup>16</sup>M. Godlewski, Phys. Rev. B **32**, 8162 (1985).
- <sup>17</sup>D. Curie and J. S. Prener, in *Physics and Chemistry of II-VI Compounds*, edited by M. Aven and J. S. Prener (North-Holland, Amsterdam, 1967), Chap. 9.
- <sup>18</sup>F. Morehead, J. Phys. Chem. Solids **24**, 37 (1963).
- <sup>19</sup>M. Godlewski, W. E. Lamb, and B. C. Cavenett, J. Lumin. **24/25**, 173 (1981).
- <sup>20</sup>M. Godlewski, W. E. Lamb, and B. C. Cavenett, Solid State Commun. **39**, 595 (1981).
- <sup>21</sup>A. Zakrzewski and M. Godlewski, Phys. Rev. B **34**, 8993 (1986).
- <sup>22</sup>A. Zakrzewski and M. Godlewski, Appl. Surf. Sci. **50**, 257 (1991).
- <sup>23</sup>T. M. Searle, Philos. Mag. B **46**, 163 (1982).